



Validity of the estimators of primary energy in giant EAS

J.-N. Capdevielle, F. Cohen

► **To cite this version:**

J.-N. Capdevielle, F. Cohen. Validity of the estimators of primary energy in giant EAS. 29th International Cosmic Ray Conference - ICRC 2005, 2005, Pune, India. International Union of Pure and Applied Physics, 7 (7), pp.59-62, 2005. <in2p3-00085920>

HAL Id: in2p3-00085920

<http://hal.in2p3.fr/in2p3-00085920>

Submitted on 17 Jul 2006

HAL is a multi-disciplinary open access archive for the deposit and dissemination of scientific research documents, whether they are published or not. The documents may come from teaching and research institutions in France or abroad, or from public or private research centers.

L'archive ouverte pluridisciplinaire **HAL**, est destinée au dépôt et à la diffusion de documents scientifiques de niveau recherche, publiés ou non, émanant des établissements d'enseignement et de recherche français ou étrangers, des laboratoires publics ou privés.

Validity of the estimators of primary energy in giant EAS

J.N. Capdevielle^a, F. Cohen^a

(a) APC, College de France, 11 place M. Berthelot, 75231 Paris Cedex 05, France

Presenter: J.N. Capdevielle (capdev@cdf.in2p3.fr), fra-capdevielle-JN-abs1-he14-oral

A set of hypergeometric gaussian functions, with a consistent relation between age parameter and total size is proposed in the ultra high energy range (above 1 EeV) for electrons, and vertical equivalent muons (vem). This is an important step for a coherent interpretation of hybrid events recorded with both surface array and fluorescence telescope. Observing that the extrapolation of the original cosmic ray primary spectrum derived from the size spectrum measured in the Akeno classical EAS array coincides with the spectrum measured recently by the Hires Stereo experiment, we point out a possible overestimation of the primary energy in inclined showers of the surface arrays like AGASA; this circumstance gives more support to the GZK synopsis.

1. Introduction

Some functions are used in large surface arrays without reference to the total size or to the age parameter, giving just an interpolation between the detectors to evaluate the densities required for the estimators at 600 m or 1000 m from axis. The longitudinal age parameter associated to the numerical values obtained via EGS is derived as :

$$s = \exp\left[\frac{2}{3} \times \left\{1 + \frac{\alpha}{t} - \tau\right\}\right] \quad \text{with } \tau = \frac{t_{max}}{t} \quad \alpha = \ln \frac{N_{max}}{N_e} \quad (1)$$

(t is expressed in cascade units). The variation of age parameter and size versus depth is shown on Figure 1 for an inclination of 45° down to AUGER level. The couple (N_e, s) is especially useful in the case of hybrid events [1] at the level of the registration; it can be derived from the fluorescence measurements to start a minimisation on the densities recorded with the surface array and give a better determination of the axis position. Such minimisation is carried with the functions described hereafter.

2. Gaussian hypergeometric lateral distribution

Those functions use the hypergeometric gaussian formalism [?] under the form :

$$f(x) = g(s) x^{s-a} (x+1)^{s-b} (1+dx)^{-c} \quad (2)$$

with $a = 1.92$, $b = 3.8$, $c = 7.71$, $d = 0.00342$ (for distances r and densities Δ , $r = xr_0$ and $\Delta = \frac{N}{r_0^2} f(r)$, $r_0 = 36.8m$, N being the total size. The calculation of the HG serial is replaced by the approximation valid up to $\theta=40^\circ$: $g(s) = -0.19 + 0.969s - 0.468s^2$. This relation works also for vem's with $a = 1.94$, $b = 3.92$, $c = 2.87$, $d = 0.00562$, $r_0 = 39.2m$, $g(s)$ being replaced by $g_{vme}(s) = 1 - 0.789s + 0.133s^2$ and finally $\Delta_{vme} = \phi_1 (N_e/r_0^2) f(x)$ with $\phi_1 = 0.47$ (agreement with experimental data shown in ref [1]).

3. Primary spectra from classical and giant arrays

The good extrapolation of the spectrum obtained in Akeno with the spectrum from HIRES Stereo is shown in Figure 2. In Akeno [2], the densities were determined with a modest detector spacing (30m or 100m) and a

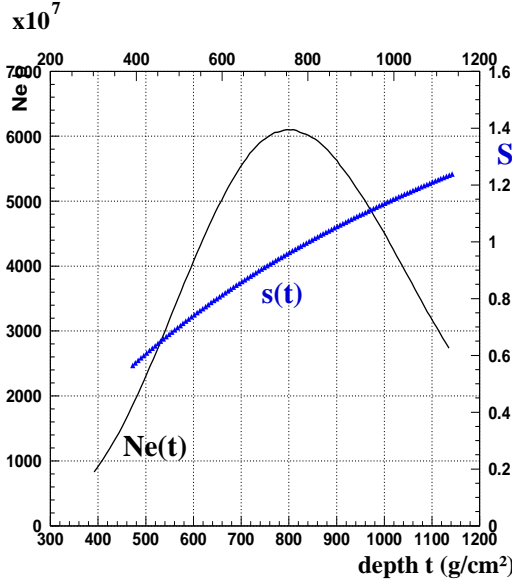


Figure 1. Longitudinal development and age parameter versus depth

specific lateral distribution, containing the age parameter was employed to localize the core and obtain the size N . The size N is converted directly to the primary energy with a relation in agreement with CORSIKA within 2% (as we have checked with QSJET option, as well as the attenuation length used for inclined showers): the differential primary flux $J(E_0)$ is then derived from the size spectrum up to $10^{18.8}$ eV. The 20 km^2 array (Array 20), prefiguring the AGASA experiment consisted of 19 detectors (individual area 2.25 m^2), separated by about 1 km from each other, uses the distribution: $\rho(r) = N C_e x^{-\alpha} (1+x)^{-(\eta-\alpha)} (1 + \frac{r}{2000})^{-0.5}$ (C_e normalisation constant). This analytic description with a fixed value $\alpha = 1.2$, without reference to the age parameter is used to determine the axis position and to interpolate the value of the density at 600m. In contrast to the size conversion in Array 1, the scintillator response in terms of density S_{600} is here converted to the primary energy following: $\bar{E}_{20}(\text{eV}) = 2.010^{17} \times (S_{600})^{1.0}$ ($S(r)$ is related to the electron and muon densities)

In place of the size spectrum, the S_{600} differential spectrum in Array 20 is obtained taking an attenuation length Λ_{600} in parallel to Λ_e in Array 1 following: $S_{600}(\Theta) = S_{600}(0) \times \exp(-\frac{t-t_0}{\Lambda_{600}})$ (3) A constant value $\Lambda_{600} = 500 \text{ g} - \text{cm}^{-2}$ was employed (also used in AGASA for $\Theta \leq 45^\circ$).

The intensity excess by a factor 1.5 of the primary spectrum appeared for Array 20 in the overlapping region with Akeno. A discrepancy by a factor 1.15 in the primary energy was observed between the respective conversions. Those ambiguities have been treated later in terms of systematic errors on detectors response versus zenith angle, seasonal variance and other complex problems related to the shower selection and the collecting area. The most recent values reported by AGASA [?] are more close from the values of Akeno than the values of Array 20 (figure 2); the intensities of AGASA remain however larger than for Array 1 in the overlapping energy region and exhibit a general excess by 30% when compared to Hires Stereo data [3]. From our simulation data, we have derived the values of the attenuation length Λ_{600} for different zenith angles: for small inclinations $\Theta \leq 30^\circ$ the values of the attenuation length concerning proton primaries are quite more important

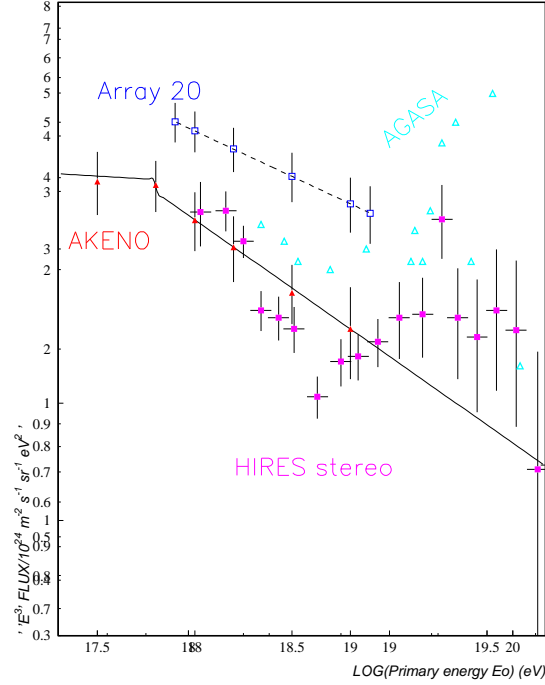


Figure 2. Differential primary spectrum for Akeno, Array 20 and Hires Stereo experiments . open square : Array 20, full triangle: Akeno, full square : Hires Stereo . The fitted spectra , for Akeno (full line) and Array 20 (dashed line) are from ref. [2] spectrum from the AGASA giant surface array (open triangles) : for the clarity of the graph, the error bars are not plotted for AGASA data.

than the average value $\Lambda_{600} = 500 \text{ g} - \text{cm}^{-2}$ used in AGASA. When the primary energy is increasing, the depth of the maximum becomes more and more close of the arrays in altitude, such as AUGER or AGASA : the conversion of inclined densities to $S_{600}(0)$ according to equation (3) becomes poorly appropriate as the cascade is far from a stable absorption phase, especially for protons primaries. In the depth interval of about 5 radiation units following the maximum, the absorption process is described by a total size N is decreasing slowly versus the atmospheric depth t , the age parameter increasing in parallel from 1.0 up to 1.2, the lateral distribution around 600 m from the axis becoming flatter. The increase of this flattening of the density distribution turns to a systematic overestimation (via relation (3)) of the vertical density and the shower recorded may be classified in bins of larger energy. Above $3.5 \cdot 10^{19} \text{ eV}$, a clear divergence in the discrepancies between AGASA and Hires Stereo appears rising from 150% above 300% at $6 \cdot 10^{19} \text{ eV}$. This may come again from the lateral distribution becoming flatter more rapidly than the reduction of the total size : the net result is that the densities (at 600 m) are 5 – 10% larger in the bin $\Theta = 20^\circ - 30^\circ$ than the vertical density when the atmospheric depth separating the array and the shower maximum becomes lower than 3 cascade units. Some systematic errors could also enter in the axis localisation.

To illustrate the complex behavior of the estimator versus zenith angle in the neighbourhood of the maximum, we have reported on table 1 the relative dependance on zenith angle at 10^{20} eV for $s(\Theta) = S_{600}(\Theta)/S_{600}(0)$ and $\delta_{vme}(\Theta) = \Delta_{vme}(\Theta)/\Delta_{vme}(0)$ in the case of water Cerenkov tanks, like in Haverah Park or AUGER, for vertical muon equivalents. This data has been obtained in a common situation at a vertical depth of $1.2 X_0$

under the maximum, X_0 being the electron radiation length for proton primaries (respectively $2.5 X_0$ for iron primaries) and allows a comparison at AUGER level ($870g - cm^{-2}$). We ascertain a maximal increase of

Table 1. Relative dependance of estimators at 600m on zenith angle for proton and iron primaries at 10^{20} eV.

Θ	0°	10°	20°	30°	40°	50°
$s(\Theta)$, p	1.	1.05	1.08	1.17	1.0	0.65
$s(\Theta)$, Fe	1.	1.007	1.012	0.94	0.80	0.47
$\delta_{vme}(\Theta)$, p	1.	1.06	1.09	1.126	1.024	0.70
$\delta_{vme}(\Theta)$, Fe	1.	1.01	1.011	0.97	0.83	0.53

the densities near 30° for the protons by 17% for scintillators and by 12.6 % for water Cerenkov tanks (those proportions are average quantities on groups of 40 showers). This can be the origin of an overestimation of the primary energy in comparable proportions.

For iron primaries, the situation is more stable but the average excess in vertical density, $S_{600}(0)$ or $\Delta_{vme}(0)$, is respectively 26% and 30% against protons: this discrepancy decreases when Θ increases with similar values of the estimators at 30° for scintillators and at 45° for the water Cerenkov tanks. The conversion to the primary energy for scintillators is then comparable for protons and heavy primaries only near 30° ; the relation(3) provides an inappropriate description for the absorption generating an energy overestimation for protons in the band 10° - 40° and a constant overestimation up to 30° for iron primaries.

Other localisations of the estimators at 800m or 1000m do not change the situation for a heavy primary component ; $s(0)$ and $\delta_{vme}(0)$ are increasing similarly, by 26% and 30% respectively at each distance, when passing from proton to iron. Furthermore, for iron, s and δ_{vme} do not depend on Θ up to 30° .

In the case of protons, the maximal enhancement near 30° appears reduced at 800m from the axis (11% for both s and δ_{vme} instead of 26% at 1000m) . For giant showers and detectors separation by 1000m or more, the accuracy on the density interpolation might be improved (a larger number of detectors hit at distances lower than 800m) and there could be some advantages to move the estimator at 800m.

4. Conclusions

The present approach points out a better consistence between the spectra obtained by classical size measurements and Hires Stereo measurements, favourable to the GZK prediction. Further simulations with CORSIKA to estimate more carefully the array response with a large statistics, completed by simulations with GEANT for the scintillator reponse and carried in close contact with the experience, may help to clarify in detail the discrepancies between the Surface arrays and the fluorescence observatories. The spectrum measured by the array KASCADE-Grande will be useful to improve the calibration of giant surface arrays.

References

- [1] J. N. Capdevielle and F. Cohen, J.Phys. G, Nucl. Part. Phys.,31, 507-524 (2005) and ref herein.
- [2] M. Nagano et al., J.Phys.G, Nucl.Part.Phys., 18, 423 (1992)
- [3] A.V. Olinto, Proc. 28th ICRC,Tsukuba, 8, 299 (2003) and ref. herein